Critical Threshold Behavior of Fluid Transport in Granular Antarctic Sea Ice

K. M. Golden[1], A. Gully[1], C. Sampson[1], D. Lubbers[2], and J. L. Tison[3]

[1]University of Utah, Department of Mathematics, 155 S 1400 E RM 233, Salt Lake City, UT 84112-0090 USA
[2]University of Utah, Department of Electrical Engineering
[3]Laboratoire de Glaciologie, CP 160/03, Université Libre de Bruxelles, 50, av. F. D. Roosevelt, 1050 - Bruxelles, Belgium

Abstract

The fluid permeability of sea ice governs a broad range of physical and biological processes in the polar marine environment. For example, in the Arctic, melt pond drainage is largely controlled by the fluid permeability of the ice. Melt ponds in turn have a significant effect on ice albedo, a critical parameter in climate models. Algae in the ice depend on nutrients from the ocean transported through the porous microstructure of sea ice when it is permeable. Columnar sea ice is effectively impermeable for brine volume fractions below about 5%, while above this threshold fluid can flow through the ice. In the Antarctic, granular ice, with a much different crystallographic structure, makes up a significant portion of the ice pack. Data gathered during SIPEX II in 2012, as well as mathematical models, indicate that the percolation threshold for the fluid permeability of granular sea ice is around 10%. This is significantly higher than for columnar ice. These findings are significant, as both ecological models involving nutrient transport and physical process models must take this into account, for example, modeling snow-ice formation, an important component of ice production in the Southern Ocean.

1 Introduction

The polar sea ice packs are a key component of the global climate system and are sensitive indicators of climate change. They also host extensive algal and bacterial communities that sustain life in the polar oceans. In addition, they play a major role in regulating gas exchanges in the polar regions and are an important factor in the Earth's overall albedo, all of which are important parameters in global and polar climate models. Fluid flow through the porous structure of sea

ice is an integral component of these important processes and properties of the ice. It also serves as the mechanism for the nutrient replenishment necessary to sustain the algal and bacterial communities which live in the ice. The ability of fluid to flow in the ice depends heavily on its microstructure and exhibits critical behavior in relation to both its crystallographic structure and brine volume fraction. Previously it was believed that granular ice was permeable for brine volume fractions above 5%, a value used in many current sea ice models. While this is the critical threshold for columnar ice, we find that it is not so for granular ice. Along with a theoretical prediction of the critical threshold, we present the first measurements of the permeability of Antarctic sea ice and show that for granular sea ice, which makes up nearly 40% of Antarctic sea ice, the critical threshold is much higher at 10%. This new result must be considered for any model in which fluid flow through sea ice is a factor.

Our focus here is on key sea ice processes that must be better understood to improve the predictions of climate models and the future of the polar icepacks, as well as the microbial communities that live there. In particular, fluid flow through porous sea ice is a major controlling component in the evolution of melt ponds which in turn affects the ice pack albedo [5], brine drainage and the evolution of salinity profiles [4, 34], snow ice formation, where sea water floods the ice surface and then freezes [22, 27], ocean-ice-atmosphere CO_2 exchanges [29], convection-enhanced thermal transport [21, 33], and biomass build-up fueled by nutrient fluxes [3, 9, 20, 30]. For example, it is believed that ice albedo feedback has played a significant role in the declines observed in the Arctic [26]. Snow-ice formation, on the other hand, may have played a part in thickening the Antarctic sea ice pack [22, 27], and may become more important in the Arctic with increased precipitation and thinning ice, making the ice more susceptible to flooding.

The fluid permeability of sea ice plays a key role in understanding such processes, and in parameterizing them in large-scale models. To date, columnar microstructures have received disproportionate attention, mostly due to their prevalence in Arctic sea ice and their importance in undisturbed ice growth [4, 19, 34]. However, granular microstructures, which lack intragranular inclusions and exhibit a film of brine enveloping individual grains, are particularly important for processes which are relevant to climate studies. For example, granular ice is common in surface layers in the Arctic [24, 25], which directly underlie the melt ponds controlling ice albedo. Examination of the crystalline structure in sea ice from a recent trans-Arctic survey [25] showed a striking increase in overall granular ice fraction, of just over 40% compared to previous observations of around 10% [15]. In the Antarctic it has long been observed that granular ice [6, 22, 16, 35] accounts for up to 40% of the sea ice pack. Snow-ice in particular, with a granular microstructure itself, accounts for over a quarter of the ice found in the Southern Ocean, with much higher fraction in some regions [23]. An accurate accounting of sea ice processes involving fluid flow in climate, biological, and biogeochemical models thusly relies on knowledge of fluid permeability of granular ice.

Golden et al. have observed that for brine volume fractions ϕ below ap-

proximately 5%, columnar sea ice is effectively impermeable to fluid flow, yet increasingly permeable for ϕ above 5% [11]. For a typical bulk salinity of 5ppt this critical brine volume fraction $\phi_c \approx 5\%$ corresponds to a critical temperature $T_c \approx -5^\circ$ C, which is known as the *rule of fives*. The critical brine volume fraction was explained in terms of the *percolation threshold* in a continuum model for compressed powders which has been used to understand the behavior of stealthy or radar absorbing materials. A comprehensive theory for the vertical fluid permeability $k(\phi)$ of columnar sea ice was developed, and validated experimentally with laboratory and Arctic field data in [12]. Microscale imaging methods based on X-ray computed tomography (CT) and pore structure analysis methods were also developed to provide detailed pictures of the brine microstructure and the evolution of its connectivity with temperature [12, 28].

During September and October of 2012, we measured the fluid permeability of first year Antarctic pack ice as participants in the Australian Sea Ice Physics and Ecosystem Experiment II (SIPEXII) aboard the ice breaker *Aurora Australis* off the east coast of Antarctica. Over 100 measurements of the fluid permeability of the ice were made covering a range of depths, temperatures and ice types. Full crystallographic cores were also taken at each site in order to correlate ice type to specific permeability measurements. The measurements corresponding to granular ice were then separated out. We found that the critical threshold for fluid flow in granular ice was around $\phi_c \approx 10\%$. For a typical salinity of around 5ppt, the corresponding critical temperature is around $T_c \approx -2.5^\circ$C [7]. Moreover as predicted by our percolation theoretic analysis in [12], we find here that the *universal* lattice critical exponent of about 2 for columnar ice in the Arctic still accurately describes the take-off of $k(\phi)$ above the threshold ϕ_c.

The behavior we find in the percolation threshold for fluid transport in granular ice is explained by the compressed power model [17, 18]. By measuring the relative dimensions of the ice grains and the fluid inclusions in photomicrographs of granular sea ice, we obtain a percolation threshold of around 10% with the possibility of even higher thresholds for more finely grained microstructures.

In conjunction with our measurements from SIPEX II in 2012 the same critical threshold can be observed in tracer experiments from SIPEX I (September-October 2007). In the tracer experiments blocks of sea ice were extracted with a chain saw then turned upside down and dyes poured into shallow channels cut into sea ice bottom. Thin vertical slices were then cut from the blocks exposing the fluid fronts and layers of different microstructures and brine channels. The tracers easily penetrated the highly permeable bottom layer but stopped at a depth characterized by a brine volume fraction of about 10% shown in Figure 1.

2 Theory

In previous work [12, 13] we found rigorous upper bounds for k based on an observed lognormal distribution for the horizontal cross-sectional areas A of the

brine inclusions [24]. In this case $Z = \ln A$ has a normal probability density with mean μ and variance σ^2,

$$P(Z) = \frac{1}{\sqrt{2\pi\sigma^2}}\, e^{-(Z-\mu)^2/2\sigma^2}. \tag{1}$$

The cross-sectional radius $a(\phi) = 7{\times}10^{-5}{+}(1.6{\times}10^{-4})\phi$ (m) increases according to measurements of pore sizes with temperature and is given by [2, 24]. The bound is a special case of optimal void bounds [31, 32], and takes the form

$$k(\phi) \le \frac{\phi}{8\pi}\, \langle A(\phi)\rangle\, e^{\sigma^2}. \tag{2}$$

With variance $\sigma^2 \approx 1$ and $\langle A(\phi)\rangle = \pi a^2(\phi)$ as above [24], the *lognormal pipe bound* in equation (2) captures all our field data, as shown in Figure 2.

Percolation theory [10, 14, 31] can used to model transport in disordered materials where the connectedness of one phase, like brine in sea ice, dominates the effective behavior. Consider the square ($d = 2$) or cubic ($d = 3$) network of bonds joining nearest neighbor sites on the integer lattice $\mathbb{Z}^d$. The bonds are assigned fluid conductivities $\kappa_0 > 0$ (open) or 0 (closed) with probabilities p and $1 - p$. There is a critical probability p_c, $0 < p_c < 1$, called the *percolation threshold*, where an infinite, connected set of open bonds first appears. In $d = 2$, $p_c = \frac{1}{2}$, and in $d = 3$, $p_c \approx 0.25$. Let $\kappa(p)$ be the permeability of this random network in the vertical direction. For $p < p_c$, $\kappa(p) = 0$. For $p > p_c$, near the threshold $\kappa(p)$ exhibits power law behavior, $\kappa(p) \sim \kappa_0(p - p_c)^e$ as $p \to p_c^+$, where e is the permeability critical exponent. For lattices, e is believed to be *universal*, depending only on d, and is equal to t, the lattice electrical conductivity exponent [1, 11, 14, 31]. In $d = 3$, it is believed [31] that $t \approx 2.0$, and there is a rigorous bound [10] that $t \le 2$.

Although e can take non-universal values in the continuum, it was shown [14, 31] that for lognormally distributed inclusions the behavior is universal, with $e \approx 2$. The scaling factor k_0 is estimated using critical path analysis and microstructural observations [12]. Thus

$$k(\phi) \;\sim\; 3\,(\phi - \phi_c)^2 \;\times 10^{-8}\ \ \mathrm{m}^2, \quad \phi \to \phi_c^+, \tag{3}$$

with $\phi_c \approx 0.1$ for granular ice.

3 Methods

We consider low Reynolds number flow of brine of viscosity η through sea ice. The volume fractions of brine and ice are ϕ and $1-\phi$, respectively. The velocity and pressure fields in the brine satisfy the Stokes equations for incompressible fluids. Under appropriate assumptions [31], the homogenized velocity $\mathbf{v}(\mathbf{x})$ and pressure $p(\mathbf{x})$ satisfy Darcy's law and the incompressibility condition for the velocity,

$$\mathbf{v} = -\frac{1}{\eta}\,\mathbf{k}\,\nabla p, \qquad \nabla\cdot\mathbf{v} = 0, \tag{4}$$

where $\mathbf{k}$ is the permeability tensor, with vertical permeability $\mathrm{k}_{zz} = k$ in units of m^2.

The *in situ* permeability data were collected using a hydrological bail test [8], where partial cylindrical holes were drilled vertically into the sea ice, and the cores removed. Once the cores are removed, a tight fitting plastic pipe wrapped in foam (a packer) is inserted into the partial hole to block any horizontal inflow from the exposed edges. Pressure transducers were then placed at the bottom of the hole to measure the height $h(t)$ of the rising water column in meters as a function of time t in seconds. The bottom 2 cm of each partial core was used for a temperature and salinity measurement giving the brine volume fraction at the interface. The permeability of the ice underneath the borehole can be accurately estimated using the equation

$$h(t) = h(t_0)e^{-k_{exp}t(g\rho/\eta L)}, \tag{5}$$

with measured permeability k_{exp} (m^2), ice thickness beneath the borehole L (m), density ρ (kg m^{-3}), gravitational constant g (m s^{-2}), and initial time t_0. The vertical component of the permeability k can then be found using the calculations in [8] which are based on simulations of the pressure field in the ice and verified by measurement.

In order to correlate the permeability measurement with the ice type a full crystallographic core was taken at each measurement site. This core was immediately taken on board the *Aurora Australis* and a standard crystallographic analysis done in a -20° c freezer using thin sections and cross polarizing film. We then matched the depths of our permeability measurements to the corresponding depths of the crystallographic core for the site to determine the ice type. For each site permeability measurements were kept to with in 3 meters of the crystallographic core to ensure close correspondence. The data were then separated out by crystal type.

The elementary analysis of the compressed powder model [17] we used to explain the rule of fives [11] shows that granular microstructures should display higher thresholds than columnar ice.

An image of the polycrystalline microstructure of Antarctic columnar ice under cross-polarization is shown in Figure 3 (A), and an image of granular ice is shown in (B). These samples were taken in the Bellingshausen Sea in October 2007 during the Sea Ice Mass Balance in the Antarctic (SIMBA) experiment.

In order to estimate the percolation threshold ϕ_c for fluid transport in Antarctic granular ice, we use a compressed powder model [11, 17]. In this model, large polymer spheres of radius R_p are mixed with much smaller metal spheres of radius R_m, and then the mixture is compressed. The main parameter controlling the threshold is the ratio $\xi = R_p/R_m$. An approximate formula for the critical volume fraction for percolation of the small metal spheres is given by $\phi_c = (1+\xi\theta/(4X_c))^{-1}$, where θ is a reciprocal planar packing factor, and X_c is a critical surface area fraction of the larger particles which must be covered for percolation by the smaller particles [17]. Values based on microstructural analysis giving good agreement with experiments are $X_c = 0.42$ and $\theta = 1.27$.

This mixture geometry is roughly similar to the ice-brine microstructure of sea ice, where the ice grains have radius R_i and the brine inclusions have radius R_b (or half the thickness of a brine film enveloping an ice grain), with $\xi = R_i/R_b$ in this case. We have estimated a range of ξ values from photomicrographs of granular microstructures, and obtained a representative value of around $\xi \approx 12$, leading to a threshold value of around $\phi_c \approx 10\%$, as illustrated in Figure 3 (C). We remark that fine-grained columnar ice which displays geometric similarity to classic granular ice can also exhibit these higher percolation threshold values, and that even finer grained frazil microstructures will likely have even higher thresholds.

4 Results and Implications

Using the full crystallographic cores taken at each site, all with in 2-3 meters of each permeability measurement, we can match the vertical permeability measurement to ice type based on depth. In Figure 4 (A) we display the granular permeability data along with the curve in equation (3). In Figure 4 (B) we show in logarithmic variables the percolation theory prediction along with a statistical best fit and the percolation theory curve showing close agreement. There is a clear take off in permeability values for brine volume fractions above 10% while below the threshold the ice is effectively impermeable. When plotting the data in logarithmic variables it is clear that for brine volume fractions above 10% percolation theory captures the data. In fact, a statical best fit of the data produces a curve $y = 1.97x + 17.5$ while percolation theory predicts a curve of $y = 2x + 17.5$.

In Figure 1 the results of our tracer experiments are shown, where we poured fluid tracers into inverted sea ice blocks. In each case the fluid descended through a layer of highly permeable sea ice, and stopped when it reached colder, impermeable granular ice (or fine-grained columnar ice) of brine volume fraction around 10%. These experiments vividly demonstrate that the critical threshold for fluid transport in Antarctic sea ice can be much higher than the 5% brine volume fraction of classic columnar sea ice.

This work demonstrates the applicability of percolation theory to fluid flow through sea ice for ice types beyond just columnar ice and shows that consideration of the microstructure of the ice is important when modeling any process in which fluid flow through the ice is relevant. Many processes such as nutrient replenishment, gas exchange and melt pond evolution depend heavily on fluid flow through the ice and are important factors in understanding the global climate system. In order to facilitate accuracy in models for both small-scale processes and large-scale climate models the higher than 5% threshold must be considered. This is particularly true in the Antarctic where up to 40% of the ice pack is comprised of granular sea ice.

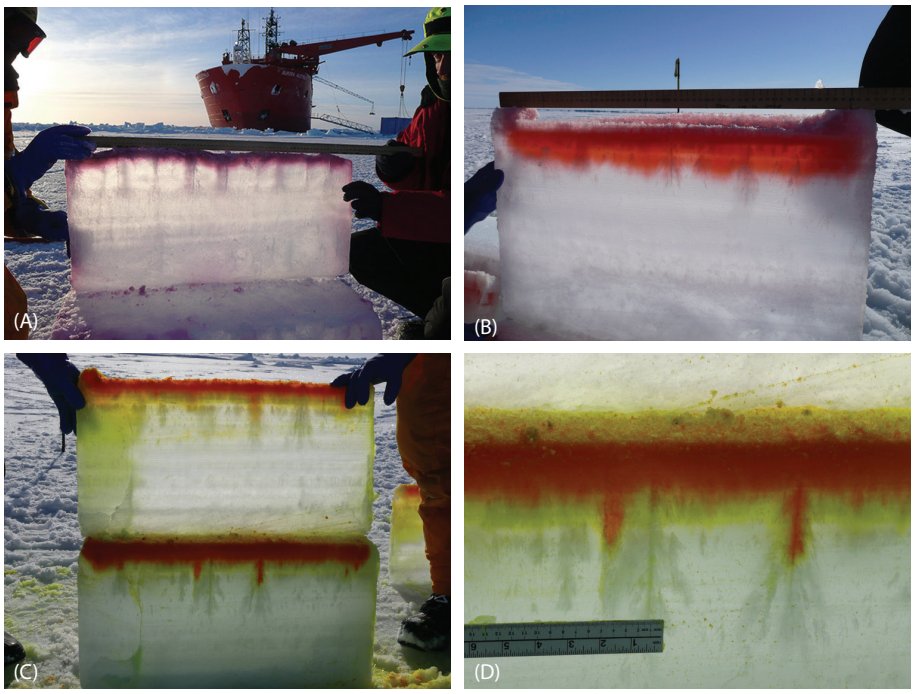

Figure 1: Penetration of tracers into inverted blocks of sea ice. The fluid penetrated about 5 cm into the ice in (a), about 10 cm in (b), and about 9 cm in (c) and (d). In each case the descending fluid passed through an initial layer a few centimeters deep of highly permeable ice of average brine volume fraction in the range 18.5% - 21.5%, until reaching relatively impermeable ice with brine volume fraction of about 10%, where it stopped flowing. In (a), the temperature and brine volume decreased more rapidly, and the tracer stopped after 5 cm. In (b) and (c) the 10% brine volume threshold was located about 10 cm down, and in (d) a tracer plume was also able to descend deeper through a large brine channel.

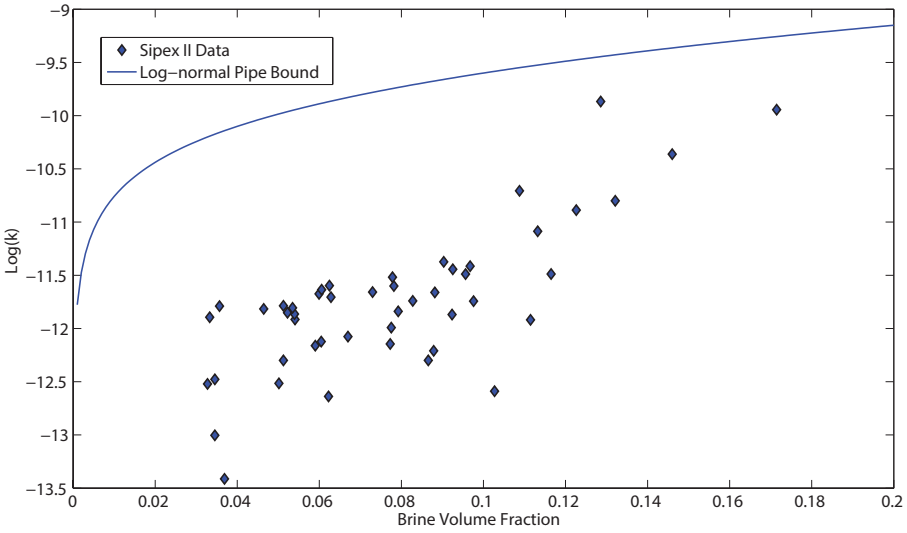

Figure 2: A comparison of *in situ* data on the vertical fluid permeability k (m^2) of Antarctic sea ice with a rigorous upper bound.

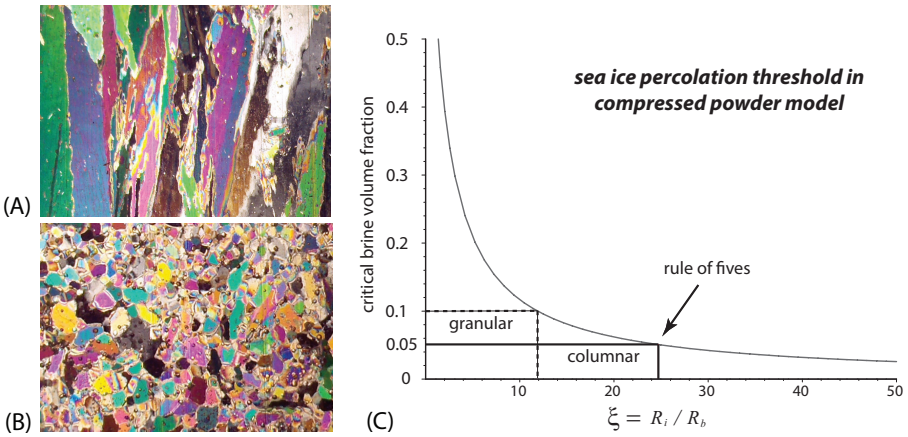

Figure 3: Examples of the different crystallographic structures of columnar and granular ice and their different permeability thresholds. Microstructures of columnar ice in (a) and granular ice in (b). In (c) we display the percolation threshold in the compressed powder model as a function of the ratio of the particle radii.

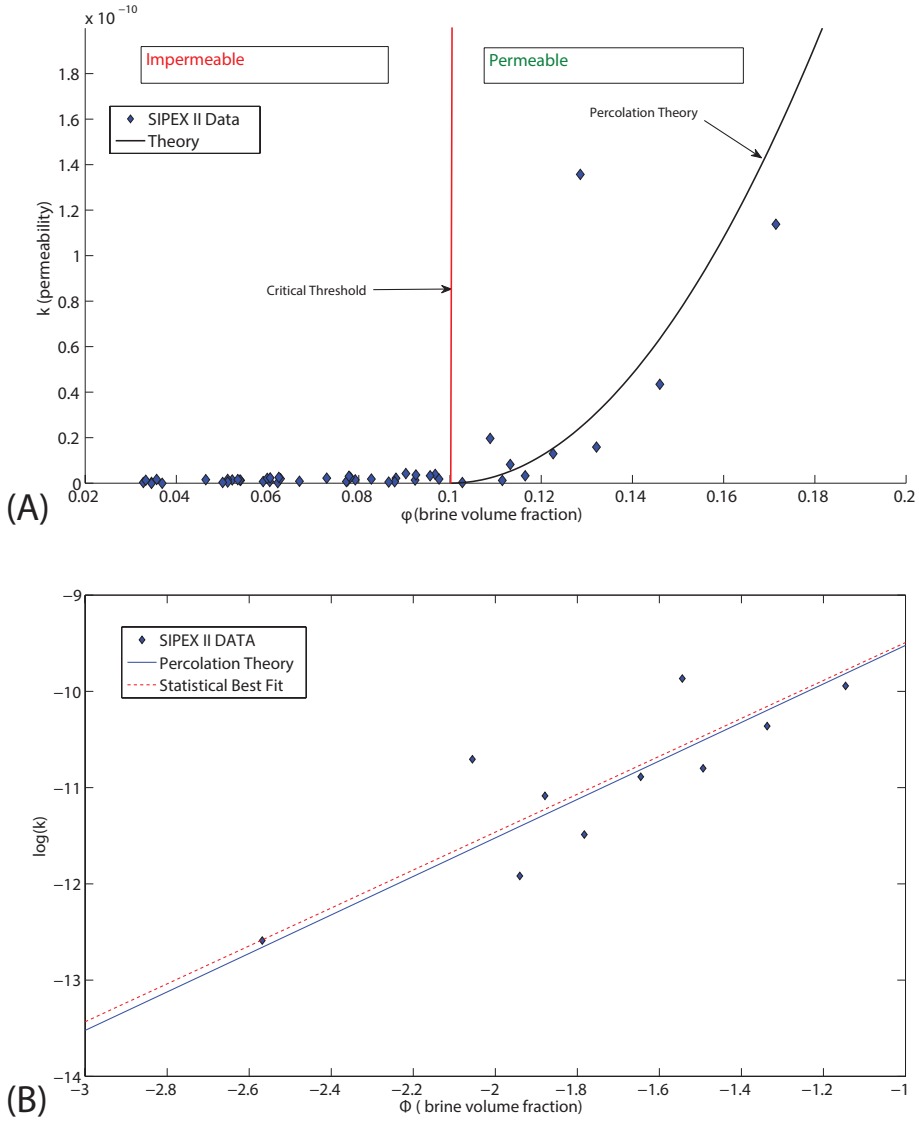

Figure 4: Comparison of *in situ* permeability data on k (m^2) for Antarctic sea ice with percolation theory. The data are displayed on a linear scale in (a) and on a logarithmic scale in (b), where a statistical best fit (dotted line) of the data is shown along with the prediction of percolation theory with $\phi_c \approx 0.1$.

References

[1] B. Berkowitz and I. Balberg. Percolation approach to the problem of hydraulic conductvity in porous media. *Transport in Porous Media*, 9:275–286, 1992.

[2] C. Bock and H. Eicken. A magnetic resonance study of temperature-dependent microstructural evolution and self-diffusion of water in Arctic first-year sea ice. *Ann. Glaciol.*, 40:179–184, 2005.

[3] H. Eicken. The role of sea ice in structuring Antarctic ecosystems. *Polar Biol.*, 12:3–13, 1992.

[4] H. Eicken. Growth, microstructure and properties of sea ice. In D. N. Thomas and G. S. Dieckmann, editors, *Sea Ice: An Introduction to its Physics, Chemistry, Biology and Geology*, pages 22–81. Blackwell, Oxford, 2003.

[5] H. Eicken, T. C. Grenfell, D. K. Perovich, J. A. Richter-Menge, and K. Frey. Hydraulic controls of summer Arctic pack ice albedo. *J. Geophys. Res. (Oceans)*, 109(C18):C08007.1–C08007.12, 2004.

[6] Hajo Eicken. *Deriving Modes and Rates of Ice Growth in the Weddell Sea from Microstructural, Salinity and Stable-Isotope Data*, pages 89–122. American Geophysical Union, 2013.

[7] G. Frankenstein and R. Garner. Equations for determing the brine volume of sea ice from -0.5^o to -22.9^o C. *J. Glaciol.*, 6(48):943–944, 1967.

[8] J. Freitag and H. Eicken. Meltwater circulation and permeability of Arctic summer sea ice derived from hydrological field experiments. *J. Glaciol.*, 49:349–358, 2003.

[9] C. H. Fritsen, V. I. Lytle, S. F. Ackley, and C. W. Sullivan. Autumn bloom of Antarctic pack-ice algae. *Science*, 266:782–784, 1994.

[10] K. Golden. Convexity and exponent inequalities for conduction near percolation. *Phys. Rev. Lett.*, 65(24):2923–2926, 1990.

[11] K. M. Golden, S. F. Ackley, and V. I. Lytle. The percolation phase transition in sea ice. *Science*, 282:2238–2241, 1998.

[12] K. M. Golden, H. Eicken, A. L. Heaton, J. Miner, D. Pringle, and J. Zhu. Thermal evolution of permeability and microstructure in sea ice. *Geophys. Res. Lett.*, 34:L16501 (6 pages and issue cover), doi:10.1029/2007GL030447, 2007.

[13] K. M. Golden, A. L. Heaton, H. Eicken, and V. I. Lytle. Void bounds for fluid transport in sea ice. *Mechanics of Materials*, 38:801–817, 2006.

[14] B. I. Halperin, S. Feng, and P. N. Sen. Differences between lattice and continuum percolation transport exponents. *Phys. Rev. Lett.*, 54(22):2391–2394, 1985.

[15] W. B. Tucker III, A. J. Gow, D. A. Meese, H. W. Bosworth, and E. Reimnitz. Physical characteristics of summer sea ice across the Arctic Ocean. *J. Geophys. Res.*, 104:1489 1504, doi:10.1029/98JC02607, 1999.

[16] M. O. Jeffries, R. A. Shaw, K. Morris, A. L. Veazey, and H. R. Krouse. Crystal structure, stable isotopes (d180), and development of sea ice in the ross, amundsen, and bellingshausen seas, antarctica. *J. Geophys. Res.*, 99:985–995, 1994.

[17] R. P. Kusy. Influence of particle size ratio on the continuity of aggregates. *J. Appl. Phys.*, 48(12):5301–5303, 1977.

[18] R. P. Kusy and D. T. Turner. Electrical resistivity of a polymeric insulator containing segregated metallic particles. *Nature*, 229:58–59, 1971.

[19] B. Light, G. A. Maykut, , and T. C. Grenfell. Effects of temperature on the microstructure of first-year Arctic sea ice. *J. Geophys. Res.*, 108(C2):3051, 2003.

[20] M. P. Lizotte and K. R. Arrigo, editors. *Antarctic Sea Ice: Biological processes, interactions and variability.* American Geophysical Union, Washington D.C., 1998.

[21] V. I. Lytle and S. F. Ackley. Heat flux through sea ice in the Western Weddell Sea: Convective and conductive transfer processes. *J. Geophys. Res.*, 101(C4):8853–8868, 1996.

[22] T. Maksym and M. O. Jeffries. A one-dimensional percolation model of flooding and snow ice formation on Antarctic sea ice. *J. Geophys. Res.*, 105(C11):26,313–26,331, 2000.

[23] T. Maksym and T. Markus. Antarctic sea ice thickness and snow-to-ice conversion from atmospheric reanalysis and passive microwave snow depth. *J. Geophys. Res.*, 113:C02S12, doi:10.1029/2006JC004085, 2008.

[24] D. K. Perovich and A. J. Gow. A quantitative description of sea ice inclusions. *J. Geophys. Res.*, 101(C8):18,327–18,343, 1996.

[25] D. K. Perovich, T. C. Grenfell, B. Light, B. C. Elder, J. Harbeck, C. Polashenski, W. B. Tucker III, and C. Stelmach. Transpolar observations of the morphological properties of Arctic sea ice. *J. Geophys. Res.*, 114:C00A04, doi:10.1029/2008JC004892, 2009.

[26] D. K. Perovich, J. A. Richter-Menge, K. F. Jones, and B. Light. Sunlight, water, and ice: Extreme Arctic sea ice melt during the summer of 2007. *Geophys. Res. Lett.*, 35:L11501, doi:10.1029/2008GL034007, 2008.

[27] D. C. Powell and T. Markus. Effects of snow depth forcing on Southern Ocean sea ice simulations. *J. Geophys. Res. C (Oceans)*, 110:C06001, doi:10.1029/2003JC002212, 2005.

[28] D. J. Pringle, J. E. Miner, H. Eicken, and K. M. Golden. Pore-space percolation in sea ice single crystals. *J. Geophys. Res. (Oceans)*, 114:C12017, 12 pp., doi:10.1029/2008JC005145, 2009.

[29] S. Rysgaard, J. Bendtsen, L. T. Pedersen, H. Ramløv, and R. N. Glud. Increased CO_2 uptake due to sea ice growth and decay in the Nordic Seas. *J. Geophys. Res.*, 114:C09011, doi:10.1029/2008JC005088, 2009.

[30] D. N. Thomas and G. S. Dieckmann, editors. *Sea Ice, 2nd Edition*. Wiley-Blackwell, Oxford, 2009.

[31] S. Torquato. *Random Heterogeneous Materials: Microstructure and Macroscopic Properties*. Springer-Verlag, New York, 2002.

[32] S. Torquato and D. C. Pham. Optimal bounds on the trapping constant and permeability of porous media. *Phys. Rev. Lett.*, 92:255505:1–4, 2004.

[33] H. J. Trodahl, M. J. McGuiness, P. J. Langhorne, K. Collins, A. E. Pantoja, I. J. Smith, and T. G. Haskell. Heat transport in McMurdo Sound first-year fast ice. *J. Geophys. Res.*, 105(C5):11347–11358, 2000.

[34] W. F. Weeks and S. F. Ackley. The growth, structure and properties of sea ice. *CRREL Monograph 82-1*, page 130 pp., 1982.

[35] A. P. Worby, Robert. Massom, and Antarctic CRC. *The structure and properties of sea ice and snow cover in East Antarctic pack ice / A.P. Worby, R.A. Massom*. Antarctic CRC Hobart, Tas, 1995.